

# Measurement of $|V_{cb}|$ and Charmless Hadronic B Decays at CLEO

XIN ZHAO\*

*Department of Physics and Astronomy  
University of Kansas, Lawrence, KS 66045 USA*

We review the recent results on the measurement of  $|V_{cb}|$  and charmless hadronic B decays from CLEO based on  $9.7 \times 10^6 B\bar{B}$  pairs collected with CLEO II and II.V detectors. The preliminary result on the measurement of  $|V_{cb}|$  is  $|V_{cb}| = (46.4 \pm 2.0 \pm 2.1 \pm 2.1) \times 10^{-3}$ . The comprehensive measurement on exclusive charmless hadronic B decays indicate existence of many contributing and interfering diagrams, especially the gluonic penguin contribution is large.

Presented at the

5th International Symposium on Radiative Corrections  
(RADCOR-2000)

Carmel CA, USA, 11–15 September, 2000

---

\*Work supported by the National Science Foundation and The Department of Energy of the United States.

## 1 CLEO experiment and CLEO III upgrade

CLEO detector has been running at the Cornell Electron Storage Ring(CESR) for 20 years, studies the B physics at the  $\Upsilon(4S)$  energy region. The CLEO II and II.V configurations are described in detail elsewhere [1,2]. It has one of the largest data sample collected at the  $\Upsilon(4S)$  region. The integrated luminosity is  $13.5 fb^{-1}$ , among them  $9.1 fb^{-1}$  taken at the  $\Upsilon(4S)$  resonance, which corresponds to about  $9.7 \times 10^6 B\bar{B}$  pairs, and  $4.4 fb^{-1}$  at the energies just below the  $B\bar{B}$  threshold in order to study backgrounds from light quark production(referred to as continuum events). The results reviewed in this paper are based on this full data sample.

Recently the CESR and CLEO detector have been upgraded. The goal is to get to a luminosity of  $1.6 - 2.2 \times 10^{33} cm^{-2} s^{-1}$ , so as to collect 20-30  $fb^{-1}$  data per year. The new CLEO III detector consists of a new four layer double sided silicon drift detector, a new 47 layer drift chamber, and a completely new barrel Ring Imaging CHernkov (RICH) detector. The upgraded detector was completed in April of 2000 and started taking physics data in July of 2000.

CLEO analysis covers wide topics in B meson decay. In this talk, we will focus on the CLEO measurements of the CKM matrix elements and CP violation.

## 2 The CKM matrix and Unitary Triangle

In the Standard Model, the Cabibbo-Kobayashi-Maskawa matrix(CKM) [3] describes the mixing between the 3 quark generations. The determination of all of these parameters is required to fully define the Standard Model and may also reveal an underlying structure that will point to new physics. In the framework of the Standard Model the CKM matrix must be unitary, which gives rise to the following relationships between the matrix elements:

$$V_{ud}V_{ub}^* + V_{cd}V_{cb}^* + V_{td}V_{tb}^* = 0, \quad (1)$$

$$V_{ub}V_{us}^* + V_{cb}V_{cs}^* + V_{tb}V_{ts}^* = 0, \quad (2)$$

$$V_{us}V_{ud}^* + V_{cs}V_{cd}^* + V_{ts}V_{td}^* = 0, \quad (3)$$

Chau, Keung [4] and Bjorken have noted that the first equation can be visualized as a triangle in the complex plane with vertices at  $(0,0)$ ,  $(0,1)$  and  $(\rho, \eta)$ . Measurements of the magnitudes of the CKM elements determine the lengths of the sides of the triangle, while measurements of the CP asymmetries determine the interior angles of the triangle. Fig. 1 shows the CKM triangle and the corresponding decay channels by which we can measure the CKM elements. The red decay modes will be discussed in this talk.

### 3 $|V_{cb}|$ from $\bar{B}^0 \rightarrow D^{*+}\ell^{-}\bar{\nu}$

The decay  $\bar{B}^0 \rightarrow D^{*+}\ell^{-}\bar{\nu}$  supplies us with a good channel to measure the CKM element  $|V_{cb}|$ , which is vital to our understanding of the unitary triangle as it sets the scale of the entire triangle. The partial width of  $\bar{B}^0 \rightarrow D^{*+}\ell^{-}\bar{\nu}$  is proportional to  $|V_{cb}|^2$ :

$$\frac{d\Gamma}{dw} = \frac{G_F^2}{48\pi^3} |V_{cb}|^2 [\mathcal{F}(w)]^2 \mathcal{G}(w), \quad (4)$$

where:  $w = v_B \cdot v_{D^*}$  is the relativistic  $\gamma$  of  $D^*$  in the B rest frame;  $\mathcal{G}(w)$  contains kinematic factors and is known by theory;  $\mathcal{F}(w)$  is the form factor describing  $B \rightarrow D^*$  transition.

At zero recoil of  $D^*$  (i.e.  $w = 1$ ),  $\frac{d\Gamma}{dw} \propto (\mathcal{F}(1)|V_{cb}|)^2$ ,  $\mathcal{F}(1)$  can be calculated by theory like HQET (Heavy Quark Effective Theory). This point is where our analysis technique comes from.

#### 3.1 The Analysis Technique

The technique is to measure  $d\Gamma/dw$  and extrapolate to  $w = 1$  to extract  $\mathcal{F}(1)|V_{cb}|$ . For  $D^*\ell\nu$ ,  $w$  runs from 1 to 1.5. We divide it into ten bins. The signal event is full reconstructed as:  $\bar{B}^0 \rightarrow D^{*+}\ell^{-}\bar{\nu}$ ,  $D^{*+} \rightarrow D^0\pi^+$  and  $D^0 \rightarrow K^-\pi^+$ . The  $\bar{B}^0 \rightarrow D^{*+}\ell^{-}\bar{\nu}$  yield in each  $w$  bin is extracted from a likelihood fit to the  $\cos\theta_{B-D^*\ell}$  distribution (the angle between the  $D^*\ell$  combination and  $B$ ). The reason why we fit to this angular distribution is that it can well distinguish between  $\bar{B}^0 \rightarrow D^{*+}\ell^{-}\bar{\nu}$  and  $\bar{B}^0 \rightarrow D^{*+}X\ell^{-}\bar{\nu}$  background events, which include events like  $\bar{B}^0 \rightarrow D^{*+}\ell^{-}\bar{\nu}$  and  $\bar{B}^0 \rightarrow D^{*+}\pi\ell^{-}\bar{\nu}$ . Because these background events don't have zero missing mass as the signal decay, so their  $\cos\theta_{B-D^*\ell}$  distribution will be much broader than the signal  $\bar{B}^0 \rightarrow D^{*+}\ell^{-}\bar{\nu}$  decay. Fig. 2 is a representative fit plot obtained in the first  $w$  bin.

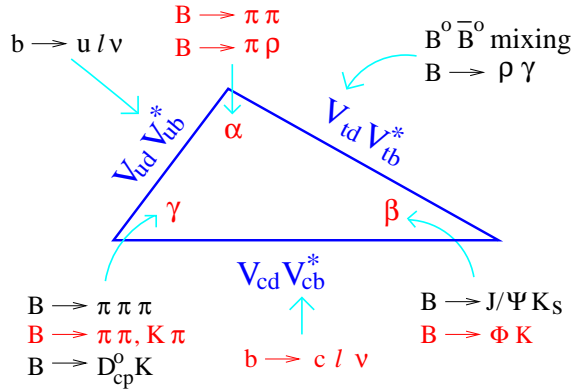


Figure 1: The unitary triangle

We then do a  $\chi^2$  fit on the overall  $w$  distribution taking into account backgrounds, reconstruction efficiency and the  $w$  resolution. We use the dispersion relations [5,6] to constrain the shapes of the form factor  $\mathcal{F}(w)$  and fit for  $\mathcal{F}(1)|V_{cb}|$  and a “slope”,  $\rho^2$  ( $atw = 1$ ), see fig. 3.

This analysis is systematic limited, the major source of uncertainty for the analysis is the efficiency for reconstructing the slow  $\pi$  from  $D^*$  decay( with systematic error of 3.1%), which is due to the uncertainties in the amount of material in the inner detector(2.3%) and the drift chamber hit efficiency(0.8%).

### 3.2 Preliminary results

We find

$$\mathcal{F}(1)|V_{cb}| = (42.4 \pm 1.8 \pm 1.9) \times 10^{-3},$$

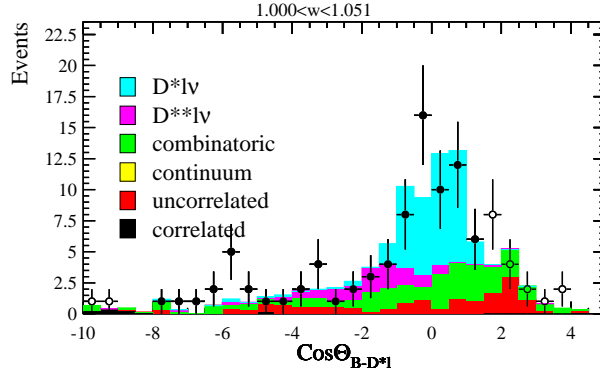


Figure 2: Fit to first  $w$  bin.

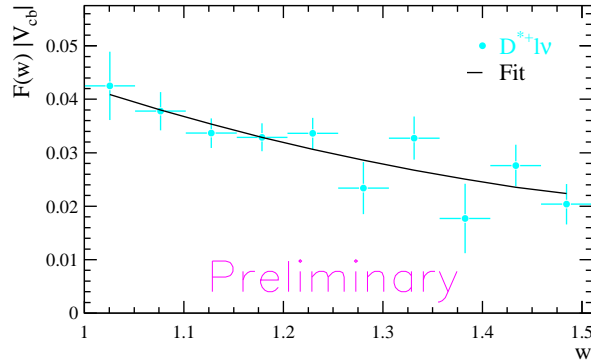


Figure 3: Fit to  $\mathcal{F}(1)|V_{cb}|$ .

$$\mathcal{B}(\overline{B}^0 \rightarrow D^{*+} \ell^- \overline{\nu}) = (5.66 \pm 0.29 \pm 0.33)\%,$$

Using  $\mathcal{F}(1) = 0.913 \pm 0.042$  [7], we calculate

$$|V_{cb}| = (46.4 \pm 2.0 \pm 2.1 \pm 2.1) \times 10^{-3},$$

This result is consistent with our previous measurements, but somewhat higher. The analysis benefits from small backgrounds and good resolution in  $w$ . A measurement using  $D^{*0} \ell \nu$  will come soon. Combining these two channels will give the best single measurement of  $|V_{cb}|$  using the exclusive technique.

## 4 Charmless Hadronic Two-Body B Decays

The rare B decays can occur through two main types of diagrams:  $b \rightarrow u$  spectator diagrams (suppressed by  $V_{ub}$ ) and  $b \rightarrow s$  penguin diagrams (suppressed by loops). Usually for one decay mode, there is more than one contributing diagrams, the interference between them gives rise to the CP violation in the B sector [8,9,10].

### 4.1 Analysis Technique

In CLEO experiment, candidates for B meson decays are distinguished from continuum background using the difference,  $\Delta E$ , between the total energy of the two tracks and the beam energy, and the beam-constrained mass,  $m_B$ . The background for rare B decays arises entirely from the continuum where the two-jet structure of the events can produce high momentum, back-to-back tracks. We suppress the continuum background via event shape because the signal events are spherical while the continuum backgrounds are jetty. Further discrimination between isotropic signal and rather jetty continuum events is provided by a Fisher discriminant technique as described in detail in Ref. [11], which is a linear combination of experimental observables.

We then perform an unbinned maximum-likelihood fit. In this fit the signal and background distributions are defined by probability density functions derived from Monte Carlo studies. The fit determines the relative contributions of the final track combinations to the signal and background. At high momentum, it's hard to separate charged K from charged  $\pi$ , so we simultaneously fit for both components, *e.g.*  $B \rightarrow K^\pm \pi^\mp / \pi^\pm \pi^\mp$ . Fig. 4 shows the fitting plots for the decay modes  $B \rightarrow K^\pm \pi^\mp / \pi^\pm \pi^\mp$ . From the contour plot (fig. 4(a)), we can see the best fit value (cross) is 4 or 5  $\sigma$  away from the point  $N_{\pi\pi} = N_{K\pi} = 0$ . The histograms in fig. 4 are projections of the fitting result onto the variables of energy difference,  $\Delta E$ , and beam constrained mass,  $M$ .

Following I will briefly review the CLEO results for the different decay modes of the charmless hadronic B decays.

## 4.2 Two body B decays to Kaons and Pions: $B \rightarrow K\pi, \pi\pi$

Ratios of various  $B \rightarrow K\pi$  branching fractions were shown [12] to depend explicitly on  $\gamma \equiv \text{Arg}(V_{ub}^*)$  with relatively modest model dependence. Within a factorization model, branching fractions of a large number of rare B decays can be parametrized by a small number of independent physical quantities, including  $\gamma$ , which can then be extracted through a global fit [13] to existing data. Finally, measurement of the time-dependent CP-violation asymmetry in the decay  $B^0 \rightarrow \pi^+\pi^-$  can be used to determine the sum of  $\gamma$  and the phase  $\beta \equiv \text{Arg}(V_{td}^*)$ .

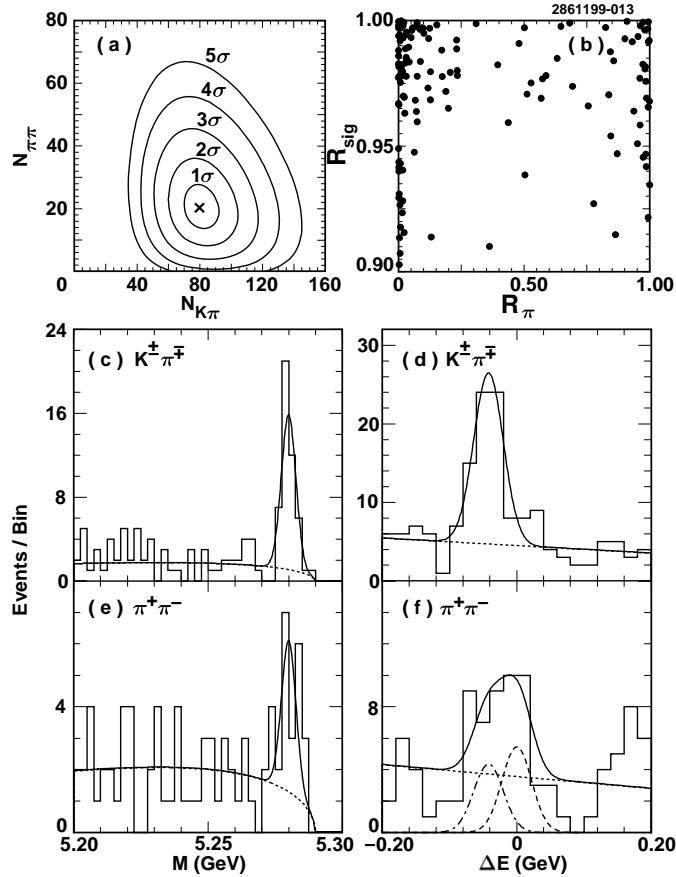


Figure 4: Illustration of Fit Results for  $B \rightarrow K^\pm\pi^\mp, \pi^\pm\pi^\mp$ . Contours of the likelihood function versus  $K\pi$  and  $\pi\pi$  event yield(a); likelihood ratios(b) - signal events cluster near the top of the figure, and separate into  $K\pi$ -like events on the left and  $\pi\pi$ -like events on the right; beam constrained mass for  $K\pi$ -like events(c);  $\Delta E$  for  $K\pi$ -like events(d); beam constrained mass for  $\pi\pi$ -like events(e);  $\Delta E$  for  $\pi\pi$ -like events(f); with both  $\pi\pi$  signal(dashed line) and  $K\pi$  cross-feed (dot-dashed line) shown.

Table 1: Measurements on  $B \rightarrow K\pi, \pi\pi$  modes (All upper limits at 90% C.L.).

Mode	$\epsilon(\%)$	Yield	Signif.	$\mathcal{B}(10^{-6})$
$K^\pm\pi^\mp$	48	$80.2^{+11.8}_{-11.0}$	$11.7\sigma$	$17.2^{+2.5}_{-2.4}\pm 1.2$
$K^0\pi^\pm$	14	$25.2^{+6.4}_{-5.6}$	$7.6\sigma$	$18.2^{+4.6}_{-4.0}\pm 1.6$
$K^\pm\pi^0$	38	$42.1^{+10.9}_{-9.9}$	$6.1\sigma$	$11.6^{+3.0+1.4}_{-2.7-1.3}$
$K^0\pi^0$	11	$16.1^{+5.9}_{-5.0}$	$4.9\sigma$	$14.6^{+5.9+2.4}_{-5.1-3.3}$
$\pi^\pm\pi^\mp$	48	$20.0^{+7.6}_{-6.5}$	$4.2\sigma$	$4.3^{+1.6}_{-1.4}\pm 0.5$
$\pi^\pm\pi^0$	39	$21.3^{+9.7}_{-8.5}$	$3.2\sigma$	$< 12.7$
$\pi^0\pi^0$	29	$6.2^{+4.8}_{-3.7}$	$2.0\sigma$	$< 5.7$
$K^\pm K^\mp$	48	$0.7^{+3.4}_{-0.7}$	$0.0\sigma$	$< 1.9$
$K^\pm K^0$	14	$1.4^{+2.4}_{-1.3}$	$1.1\sigma$	$< 5.1$
$K^0\overline{K^0}$	5	0	$0.0\sigma$	$< 17$

Table 2: Measurements on  $\eta'$  and  $\eta$  modes.

Mode	Signif.	$\mathcal{B}(10^{-6})$
$B^+ \rightarrow \eta' K^+$	$16.8\sigma$	$80^{+10}_{-9}\pm 7$
$B^0 \rightarrow \eta' K^0$	$11.7\sigma$	$89^{+18}_{-16}\pm 9$
$B^+ \rightarrow \eta K^{*+}$	$4.8\sigma$	$26.4^{+9.6}_{-8.2}\pm 3.3$
$B^0 \rightarrow \eta K^{*0}$	$5.1\sigma$	$13.8^{+5.5}_{-4.6}\pm 1.6$

Table 1 summarizes the CLEO results on the  $B \rightarrow K\pi, \pi\pi$  modes. We finally observed all four  $K\pi$  modes. For some decay modes, the significance of the signal is not enough to claim an observation of the decay modes, so we just come up with upper limits.  $B \rightarrow \pi^0\pi^0$  is a new result, while the other results are also improved to the previous ones [14]. These results can be used to set new bound on the angle  $\gamma$  of the unitary triangle [15]. They also indicate that the gluonic penguin diagram contribution to the rare B decays is large.

### 4.3 Modes with $\eta'$ and $\eta$

An earlier search [16] found a large rate for the decay  $B \rightarrow \eta' K$ , and set upper limits on other decays to two-body final states containing  $\eta'$  or  $\eta$  mesons. In table 2, we summarize the latest CLEO measurements on these decay modes, we only observe signals on these four modes shown in table 2, for other modes, there is just upper

Table 3:  $B \rightarrow PV$  Modes

Mode	Yield	Signif.	$\mathcal{B}$ ( $10^{-6}$ )
$B^- \rightarrow \pi^- \rho^0$	$29.8_{-9.6}^{+9.3}$	$5.4\sigma$	$10.4_{-3.4}^{+3.3} \pm 2.1$
$B^- \rightarrow \pi^- \omega$	$28.5_{-7.3}^{+8.2}$	$6.2\sigma$	$11.3_{-2.9}^{+3.3} \pm 1.4$
$B^0 \rightarrow \pi^\pm \rho^\mp$	$31.0_{8.3}^{+0.4}$	$5.6\sigma$	$27.6_{-7.4}^{+8.4} \pm 4.2$

limits [17]. These results confirmed the previous observations that the  $\eta'K$  signal is larger than  $\eta K$ . To explain this phenomenon, a substantial intrinsic charm component of the  $\eta'$  has been proposed [18,19], but the new CLEO results on  $B \rightarrow \eta_c K$  [20]:

$$\text{BR}(B^0 \rightarrow \eta_c K^0) = (1.09_{-0.42}^{+0.55} \pm 0.12 \pm 0.31) \times 10^{-3},$$

$$\text{BR}(B^+ \rightarrow \eta_c K^+) = (0.69_{-0.21}^{+0.26} \pm 0.08 \pm 0.20) \times 10^{-3}$$

shows no enhancement compared to the  $B \rightarrow J/\psi K$  decay.

#### 4.4 B meson decays to Pseudoscalar-Vector final states

CLEO recently made the first observation of the decays  $B^- \rightarrow \pi^- \rho^0$ ,  $B^- \rightarrow \pi^- \omega$  and  $B^0 \rightarrow \pi^\pm \rho^\mp$  (charge-conjugate modes are implied) [21], as summarized in table 3. All of these  $\Delta S=0$  decay modes are expected to be dominated by hadronic  $b \rightarrow u$  transitions. We see no significant yields in any of the  $\Delta S=1$  transitions. This is in contrast to the corresponding charmless hadronic B decays to two pseudoscalar mesons ( $B \rightarrow PP$ )  $B \rightarrow K\pi, \pi\pi$ , where  $\Delta S=1$  transitions clearly dominate. It indicates that gluonic penguin decays play less of a role in  $B \rightarrow PV$  decays than in  $B \rightarrow PP$  decays. This is consistent with theoretical predictions [22] that uses factorization which predicts destructive (constructive) interference between penguin operators of opposite chirality for  $B \rightarrow K\rho$  ( $B \rightarrow K\pi$ ), leading to a rather small (large) penguin contribution in these decays.

#### 4.5 Observation of $B \rightarrow \phi K$ - Preliminary

The decay  $b \rightarrow s\gamma$  produced by the gluonic penguin can be uniquely tagged when the gluon splits into an  $s\bar{s}$  pair as no other b decay can produce this final state. The mode  $B \rightarrow \phi K$  is one such tag of the gluonic penguin and its rate is sensitive to  $\sin 2\beta$  in the CKM matrix. CLEO recently measured  $\text{BR}(B^- \rightarrow \phi K^-) = (6.4_{-2.1-2.0}^{+2.5+0.5}) \times 10^{-6}$  and  $\text{BR}(B^0 \rightarrow \phi K^0) = (5.9_{-2.9-0.9}^{+4.0+1.1}) \times 10^{-6}$ . Assuming that the branching ratio for these two processes should be equal, we obtain

$$\text{BR}(B \rightarrow \phi K) = (6.2_{-1.8-1.7}^{+2.0+0.7}) \times 10^{-6}$$

The first set of errors is statistical, whereas the second set is systematic, dominated by systematics of the unbinned maximum likelihood fit. While statistical significance of the signal in the  $B^- \rightarrow \phi K^-$  mode is  $4.4 \sigma$ , the statistical significance of the  $B^0 \rightarrow \phi K^0$  signal is only  $2.8\sigma$ . Thus, without any theoretical bias, we cannot claim the signal in the  $B^0 \rightarrow \phi K^0$  mode with high confidence and therefore we calculate the upper limit of  $< 1.2 \times 10^{-5}$  at 90% C.L. The signal significance in the combined charged and neutral kaon data is well above 5 standard deviations.

#### 4.6 CP Asymmetry Measurements

Direct CP asymmetry can result from interference of two amplitudes with different strong and weak phases. The asymmetry,  $\mathcal{A}_{CP}$  is defined by the difference between the rates for  $\overline{B} \rightarrow f$  and  $B \rightarrow \overline{f}$  as

$$\mathcal{A}_{CP} \equiv \frac{\mathcal{B}(\overline{B} \rightarrow f) - \mathcal{B}(B \rightarrow \overline{f})}{\mathcal{B}(\overline{B} \rightarrow f) + \mathcal{B}(B \rightarrow \overline{f})}, \quad (5)$$

Precise predictions for  $\mathcal{A}_{CP}$  are not feasible at present as both the absolute value and the strong interaction phases of the contributing amplitudes are not calculable. However, numerical estimates can be made under well-defined model assumptions and the dependence on both model parameters and CKM parameters can be probed. Recent calculations of CP asymmetries under the assumption of factorization have been published by Ali et al. [23].

In table 4, we present results [24] of searches for CP violation in decays of B mesons to the three  $K\pi$  modes,  $K^\pm\pi^\mp$ ,  $K^\pm\pi^0$ ,  $K^0\pi^\pm$ , the mode  $K^\pm\eta'$ , and the vector-pseudoscalar mode  $\omega\pi^\pm$ . These decay modes are selected because they have well measured branching ratios and significant signal yields in our data sample [17,14,21]. In the data analysis, these decays are self-tagging, the flavor of the parent  $b$  or  $\overline{b}$  quark is tagged simply by the sign of the high momentum charged hadron. The asymmetry,  $\mathcal{A}_{CP}$ , is obtained from the maximum likelihood fit as a free parameter.

We see no evidence for CP violation in the five modes and set 90% CL intervals that reduce the possible range of  $\mathcal{A}_{CP}$  by as much as a factor of four. While the sensitivity is not yet sufficient to probe the rather small  $\mathcal{A}_{CP}$  values predicted by factorization models, extremely large  $\mathcal{A}_{CP}$  values that might arise if large strong phase differences were available from final state interactions are firmly ruled out. For the cases of  $K\pi$  and  $\eta'K$ , we can exclude  $|\mathcal{A}_{CP}|$  greater than 0.30 and 0.23 at 90% CL respectively.

## 5 Conclusions

Besides the results discussed above, CLEO has also many other physics results for B decay at  $\Upsilon(4S)$ . However, the unambiguous observation of the gluonic penguin

Table 4: CP asymmetry measurements from CLEO

Mode	Yield	$\mathcal{A}_{CP}$
$K^\pm\pi^\mp$	$80.2^{+11.8}_{-11.0}$	$-0.04 \pm 0.16$
$K^\pm\pi^0$	$42.1^{+10.9}_{-9.9}$	$-0.29 \pm 0.23$
$K^0\pi^\pm$	$25.2^{+6.4}_{-5.6}$	$+0.18 \pm 0.24$
$K^\pm\eta'$	$100^{+13}_{-12}$	$+0.03 \pm 0.12$
$\omega\pi^\pm$	$28.5^{+8.2}_{-7.3}$	$-0.34 \pm 0.25$

and the best single measure of  $|V_{cb}|$  are undoubtedly the highlights in the last year. As the CLEO III starts data taking and the asymmetric B factories gets their first results, we can all look forward to much more exciting physics from the  $\Upsilon(4S)$  in the future.

## Acknowledgments

I am grateful to Alice Bean, Karl Ecklund and the other CLEO and Kansas colleagues for the helpful discussions in preparing for the talk.

## References

- [1] CLEO Collaboration, Y.Kubota *et al.*, *Nucl. Instrum. Methods* **A320**,(1992)66.
- [2] T. Hill, *Nucl. Instrum. Methods* **A418**,(1998)32.
- [3] M. Kobayashi and T. Maskawa, *Progr. Theor. Phys.* **49**,(1973)652.
- [4] L.L.Chau and W.Y.Keung, *Phys. Rev. Lett.* **53**,(1984)1802.
- [5] I. Caprini,L. Lellouch and M. Neubert, *Nucl. Phys.* **B530** (1998)153;
- [6] C.G. Boyd, B. Grinstein and R.F. Lebed, *Phys. Rev.* **D56** (1997)6895;
- [7] BaBar Physics Book, P.F. Harrison and H.R.Quinn ed. *SLAC-R-504* (1998);
- [8] A.J.Buras, Lectures given at the 14th Lake Louise Winter Institute, *hep-ph/9905437*(February, 1999);

- [9] M.Neubert and J.L.Rosner, *Phys. Rev. Lett.* **81** (1998)5076;*Phys. Lett.* **B441**(1998)403
- [10] M.Bander, D.Silverman and A.Soni, *Phys. Rev. Lett.* **43** (1979)242;
- [11] D.M.Asner *et al.*(CLEO Collaboration) *Phys. Rev.* **D53** (1996)1039;
- [12] M.Gronau, J.L.Rosner, and D.London, *Phys. Rev. Lett.* **73** (1994)21;  
R.Fleischer, *Phys. Lett.* **B365** (1996)399; R.Fleischer, and T.Mannel, *Phys. Rev.* **D57** (1998)2752.
- [13] W.-S. Hou,J.G.Smith and F.Wurthwein, *hep-ex/9910014*.
- [14] D. Cronin-hennessy *et al.* (CLEO Collaboration) *Phys. Rev. Lett.* **85**,(2000)515
- [15] M.Neubert,J.L.Rosner, *Phys. Lett.* **B441** (1998)403.
- [16] B.H.Behrens, *et al.* (CLEO Collaboration) *Phys. Rev. Lett.* **80** (1998)3710.
- [17] S.J.Richichi, *et al.* (CLEO Collaboration) *Phys. Rev. Lett.* **85** (2000)525.
- [18] I.Halperin and A.Zhitnitsky, *Phys. Rev.* **D56** (1997)7247; E.V.Shuryak and A.R.Zhitnitsky *Phys. Rev.* **D57** (1998)2001.
- [19] F.Yuan and K.-T. Chao, *Phys. Rev.* **D56** (1997)2495.
- [20] K.W.Edwards *et al.* (CLEO Collaboration) *Phys. Rev. Lett.* **86** (2001)30.
- [21] C.P. Jessop, *et al.* (CLEO Collaboration) *Phys. Rev. Lett.* **85** (2000)3095.
- [22] K. Lingel, T.Skwarnicki, J.G.Smith, *Ann. Rev. Nucl. Part. Sci.***48** (1998)253;  
Y-H Chen, H-Y Cheng, B.Tseng and K-C Yang, *Phys. Rev.***D60** (1999)094014.
- [23] A.Ali,G.Kramer and C.D.Lu, *Phys. Rev.***D59** (1999)014005.
- [24] S.Chen *et al.* (CLEO Collaboration) *Phys. Rev. Lett.* **85** (2000)525.